

# Part 3 REFLECTION AND TRANSMISSION OF ULTRASONIC WAVES

Nearly all applications of ultrasonics involve the interaction of waves with boundaries. Nondestructive testing, medical imaging and sonar are ready examples of this. Even basic studies of material properties, usually involving the attenuation of waves, require in the final analysis accounting for boundary interactions.

## 3.1 Reflection/transmission - normal incidence

The simplest situation of reflection and transmission occurs when waves are impinging normal to the surface. In Fig. 3.1, the case of a longitudinal wave incident on the interface between two media is shown. This situation may be described mathematically in terms of three propagating waves

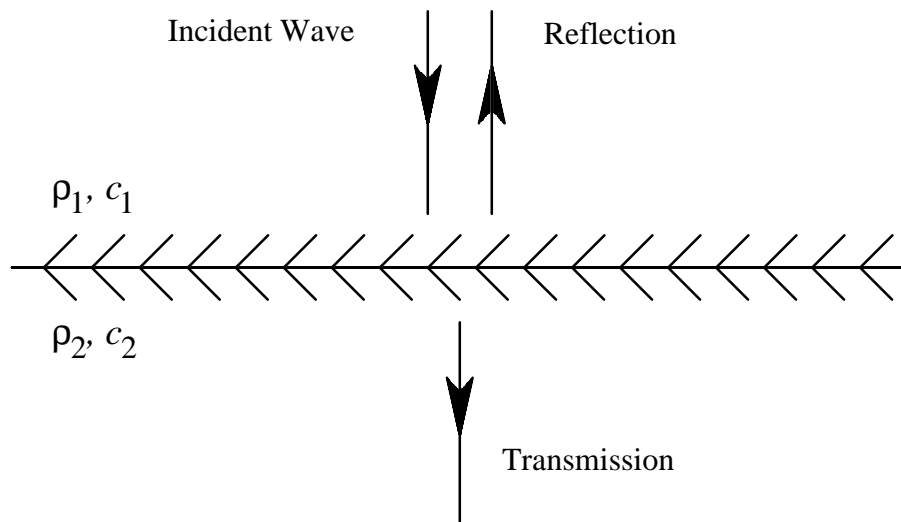


Figure 3.1 Reflection and transmission of an acoustic wave at normal incidence to a plane boundary.

$$u_i = A_i \sin(k_1 x - \omega t), \quad (3.1)$$

$$u_r = -A_r \sin[-(k_1 x + \omega t)], \quad (3.2)$$

$$u_t = A_t \sin(k_2 x - \omega t). \quad (3.3)$$

The amplitude of the reflected and transmitted waves may be found by noting that the displacements and stresses must be the same (continuous) at the interface. Thus, for  $x = 0$ , it is required that

$$u_i + u_r = u_t \quad \text{and} \quad \tau_i + \tau_r = \tau_t. \quad (3.4)$$

This leads directly to the result

$$R_d = \frac{A_r}{A_i} = \frac{\rho_2 c_2 - \rho_1 c_1}{\rho_1 c_1 + \rho_2 c_2} \quad (3.5)$$

and

$$T_d = \frac{A_t}{A_i} = \frac{2\rho_1 c_1}{\rho_1 c_1 + \rho_2 c_2}. \quad (3.6)$$

This gives the ratio of the displacement amplitude. More commonly, the stress (or pressure) amplitudes are given. Thus,

$$R_s = \frac{\tau_r}{\tau_i} = \frac{\rho_2 c_2 - \rho_1 c_1}{\rho_1 c_1 + \rho_2 c_2} = R_d \quad (3.7)$$

and

$$T_s = \frac{\tau_t}{\tau_i} = \frac{2\rho_2 c_2}{\rho_1 c_1 + \rho_2 c_2} \neq T_d, \quad (3.8)$$

where  $R$  and  $T$  are known as the *reflection* and *transmission* coefficients. It is seen that these results are in terms of the respective acoustic impedances of the materials.

Illustration of the reflection and transmission at various interface combinations are worth considering. For *steel-water*, we have  $\rho_s c_s = 46.5 \times 10^6 \text{ kg/m}^2\text{s}$  and  $\rho_w c_w = 1.5 \times 10^6 \text{ kg/m}^2\text{s}$ . From Eqs. 3.7 and 3.8, one obtains  $R = -0.938$  and  $T = 0.063$ . The interpretation of this result is that the amplitude of the reflected stress wave is 0.938 (or 93.8%) that of the incident amplitude. The negative sign indicates that the reflected wave is 180° out of phase with the incident wave. Thus, when the incident wave is compressive, the reflected wave is tensile and vice-versa. The transmitted pressure amplitude is but 6.3% of the incident amplitude. This reflection/transmission situation is shown in Fig. 3.2a. For *water-steel*, by using the previous values for  $\rho_s c_s$ ,  $\rho_w$ , and  $c_w$ , we obtain from Eqs. 3.7 and 3.8  $R = 0.938$  and  $T = 1.938$ . Thus, the reflected wave amplitude is nearly the same as the incident amplitude, where the transmitted (stress) amplitude is nearly twice the incident amplitude, as shown in Fig. 3.2b.

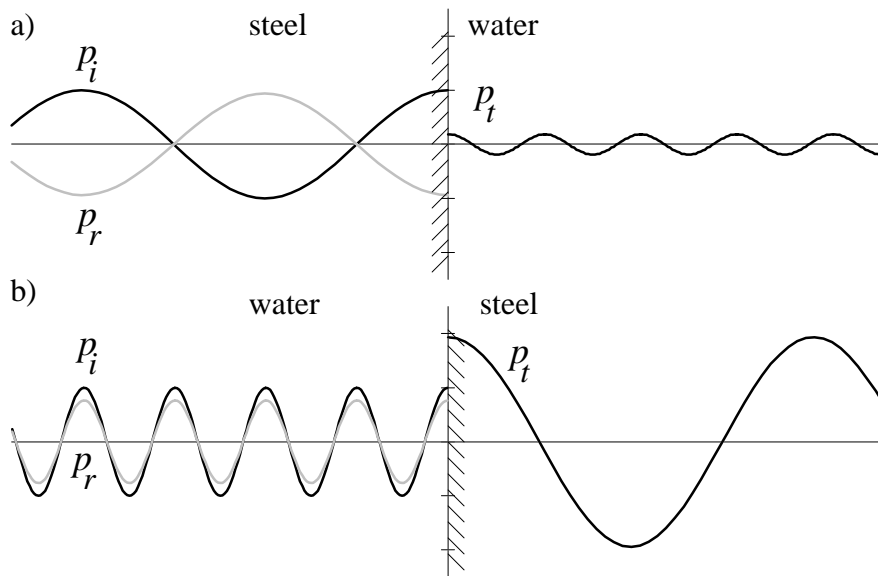


Figure 3.2 Sound pressure values in the case of reflection from (a) a steel-water and (b) a water-steel interface at normal incidence.

The preceding result may appear strange, as though conservation of energy were being violated. However, both wave amplitude and wave velocity determine the time rate of flow of energy (i. e., power) at the interface. In terms of power, there should be a net balance. That is,

$$P_r + P_t = P_i \quad (3.9)$$

should be satisfied. The power per unit area (i. e., intensity) will be given by  $I = -\tau v$ , where  $\tau = C_{11} \partial u / \partial x$  and  $v = \partial u / \partial t$ . Using Eqs. 3.1-3.3 to calculate  $P_i, P_r, P_t$  and substituting in the power balance expression shows it to be satisfied.

*Special cases:* Suppose media 2 is vacuum, so that  $\rho_2 c_2 = 0$ . One obtains

$$R_d^{free} = -1, \quad T_d^{free} = 2, \quad R_s^{free} = -1, \quad \text{and} \quad T_s^{free} = 0$$

indicating a simple phase reversal of the incident wave. Suppose media 2 is infinitely rigid, so that  $\rho_2 c_2 \rightarrow \infty$ . Then from Eqs. 3.5 through 3.8 one obtains

$$R_d^{clamped} = 1, \quad T_d^{clamped} = 0, \quad R_s^{clamped} = 1, \quad \text{and} \quad T_s^{clamped} = 2$$

There is thus no phase reversal of the incident displacement wave.

The case of shear waves normally incident on a boundary may also be considered. However, a small subtlety arises. If the two media are bonded together, then conditions at the interface would be that  $v_i + v_r = v_t$ ,  $\tau_i + \tau_r = \tau_t$ , and expressions of the form Eqs. 3.5 through 3.8 would be obtained, with all velocities merely being changed to shear wave velocities. However, the more common cases of a fluid-solid interface or of two solids separated by a thin film of lubricant would prevent transmission of shear waves across the interface.

The case of waves normally incident on a layer sandwiched between two media is the next step of complexity and represents a situation frequently arising in ultrasonics. Reflection at and transmission through an elastic layer exhibit strong frequency dependence associated with resonances in the layer. One of the simplest approach to describe this problem is applying the *impedance-translation theorem* to the layer [See for example, L. M. Brekhovskikh, *Waves in Layered Media* (Academic, New York, 1980) pp. 23-26]. The *impedance-translation theorem* says that the input impedance  $Z_{input}$  of a layer can be calculated from the loading impedance  $Z_{load}$  presented by the medium behind the layer and the acoustic impedance  $Z_o$  of the layer itself as follows:

$$Z_{input} = Z_o \frac{Z_{load} - iZ_o \tan(k_o d)}{Z_o - iZ_{load} \tan(k_o d)}. \quad (3.10)$$

Although this theorem is well known and widely used in several area, such as electrical engineering, it is very instructional to derive it from the boundary conditions prevailing at the two interfaces. Let us write the stress distribution in the layer in the following general form:

$$\tau(x) = A_+ \exp(ik_o x) + A_- \exp(-ik_o x), \quad (3.11)$$

which is the sum of a forward and backward propagating plane wave.  $A_+$  and  $A_-$  are the complex amplitudes of the two waves and we omitted the common  $\exp(-i\omega t)$  term. The velocity distribution is given by

$$v(x) = -\frac{\partial \tau / \partial x}{i\omega \rho_o} = -\frac{1}{Z_o} [A_+ \exp(ik_o x) - A_- \exp(-ik_o x)]. \quad (3.12)$$

The input impedance of the layer is

$$Z_{input} = -\frac{\tau(0)}{v(0)} = Z_o \frac{A_+ + A_-}{A_+ - A_-}, \quad (3.13)$$

where the ratio of the complex amplitudes  $A_+$  and  $A_-$  can be determined from the condition that

$$Z_{load} = -\frac{\tau(d)}{v(d)} = Z_o \frac{A_+ e^{ik_o d} + A_- e^{-ik_o d}}{A_+ e^{ik_o d} - A_- e^{-ik_o d}}. \quad (3.14)$$

$$\frac{A_+}{A_-} = \frac{Z_{load} e^{-ik_o d} + Z_o e^{-ik_o d}}{Z_{load} e^{ik_o d} - Z_o e^{ik_o d}} \quad (3.15)$$

Substitution of (3.15) into (3.13) yields

$$Z_{input} = Z_o \frac{Z_{load} \cos(k_o d) - iZ_o \sin(k_o d)}{Z_o \cos(k_o d) - iZ_{load} \sin(k_o d)} \quad (3.16)$$

which is identical with the previously given form of (3.10).

The reflection coefficient of the layer can be easily obtained from (3.7) as

$$R = \frac{Z_{input} - Z_1}{Z_{input} + Z_1} \quad (3.17)$$

from  $Z_{load} = Z_2$ . In the simplest case of  $Z_2 = Z_1$ , the reflection coefficient turns out to be

$$R = \frac{i \tan(k_o d)(Z_o^2 - Z_1^2)}{i \tan(k_o d)(Z_o^2 + Z_1^2) - 2Z_o Z_1}, \quad (3.18)$$

while the transmission coefficient can be calculated from the law of energy conservation as

$$|T| = \sqrt{1 - |R|^2}. \quad (3.19)$$

From Equations 3.18 and 3.19, the moduli of the reflection and transmission coefficients can be written as follows

$$|R| = \frac{\xi \sin(k_o d)}{\sqrt{\xi^2 \sin^2(k_o d) + 1}} \quad (3.20)$$

and

$$|T| = \frac{1}{\sqrt{\xi^2 \sin^2(k_o d) + 1}}, \quad (3.21)$$

where  $\xi = \frac{1}{2} |Z_o / Z_1 - Z_1 / Z_o|$  is a measure of the impedance contrast between the layer and the surrounding host materials.

The general situation is shown in Fig. 3.2a, where repeated reflections occur within the layer until a steady reflection, transmission state is reached. Not only do the material impedances enter, the ratio of layer thickness to acoustic wavelength ( $d/\lambda_o$ ) strongly influences the result, too. The particular cases of steel and Plexiglas plates in water are shown in Fig. 3.3b.

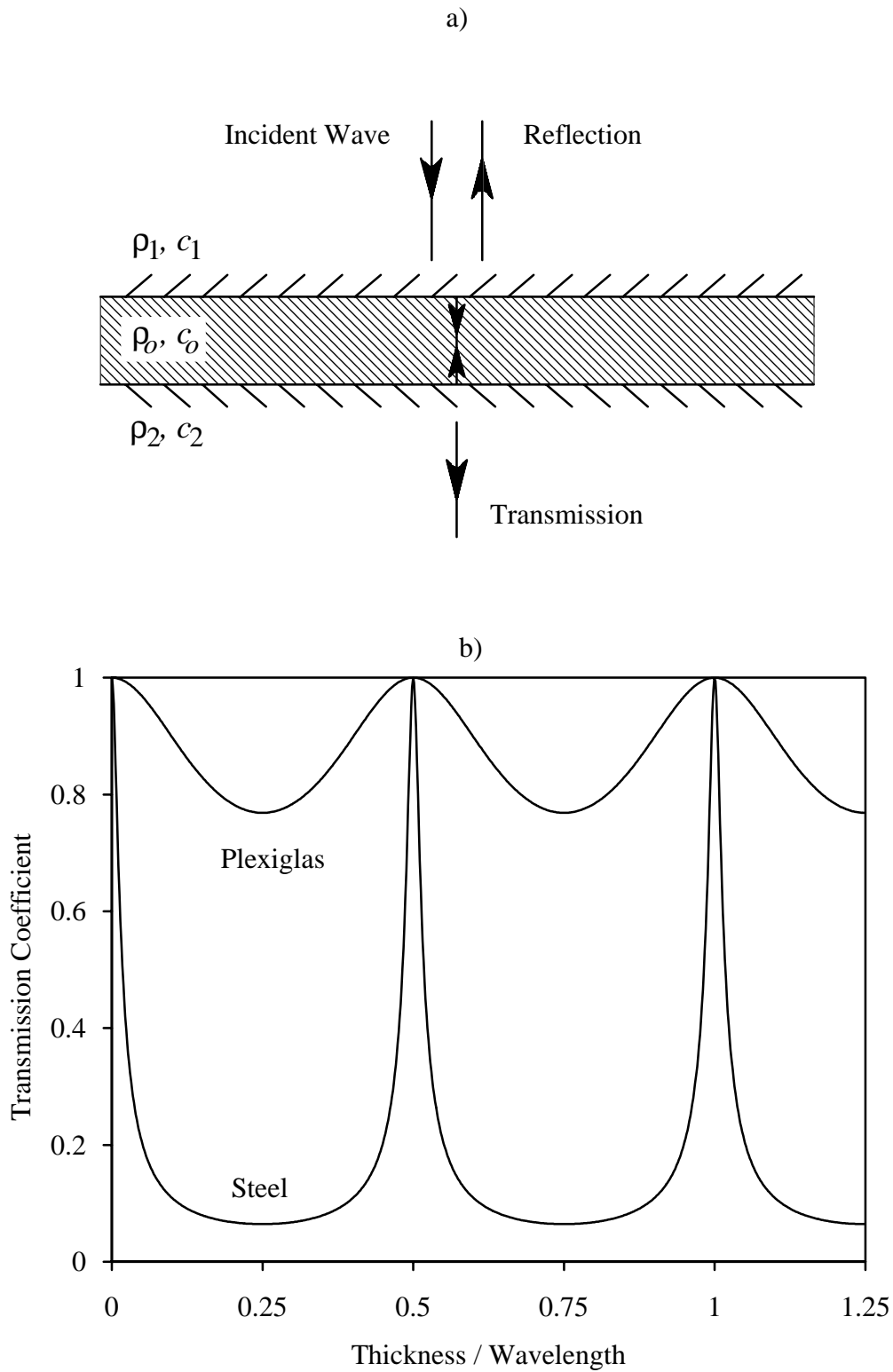


Figure 3.3 (a) Schematic diagram of reflection at and transmission through a layered medium and (b) specific cases of steel and Plexiglas plates in water.

Equation 3.20 can be used to answer one of the basic questions of ultrasonic nondestructive evaluation concerning the reflectivity of thin cracks in solids. As an example, Figure 3.4 shows the reflectivities of air-filled and water-filled cracks in steel as functions of the frequency-thickness product [J. Krautkramer and H. Krautkramer, *Ultrasonic Testing of Materials* (Springer, Berlin, 1977) p. 29]. For very thin cracks,

$$\lim_{d \rightarrow 0} |R| = \xi k_o d , \quad (3.22)$$

i. e., the reflectivity is proportional to the product of impedance mismatch, frequency, and layer thickness.

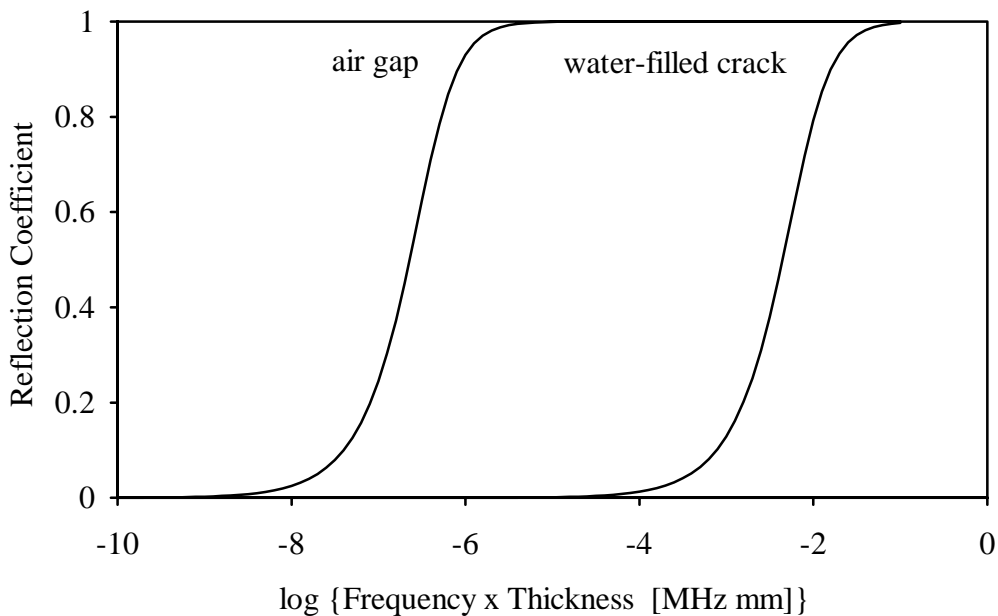


Figure 3.4 The reflectivities of air-filled and water-filled cracks in steel as functions of the frequency-thickness product.



One of the most important consequence of the impedance-translation theorem of Eq. 3.10 is the impedance matching capability of a single layer. When the layer thickness is an odd multiple of the quarter-wavelength in the layer material, i. e.,  $d = (2n+1)\lambda/4$ , the input and load impedances are related through

$$Z_{input} = \frac{Z_o^2}{Z_{load}}. \quad (3.23)$$

This means that perfect matching (total transmission and zero reflection) can be achieved even between widely different impedances if a quarter-wavelength matching layer of  $Z_o = \sqrt{Z_1 Z_2}$  acoustic impedance is applied at the interface. Let us denote the center frequency where the layer thickness equals to one quarter-wavelength by  $f_o$ . In the vicinity of this center frequency,

$$\sin(k_o d) \approx 1, \text{ and } \cos(k_o d) \approx \Delta, \text{ where } \Delta = \frac{\pi}{2} \frac{f_o - f}{f_o}, \quad (3.24)$$

and the reflection coefficient can be approximated as follows

$$R \approx \frac{r-1}{r+1 - i \frac{2\sqrt{r}}{\Delta}} \approx i\Delta \frac{r-1}{2\sqrt{r}}, \quad (3.25)$$

where  $r = Z_2/Z_1$  denotes the impedance ratio between the two media to be matched. The energy transmission coefficient through the matching layer can be approximated as

$$T_{energy} \approx 1 - \Delta^2 \frac{(r-1)^2}{4r}. \quad (3.26)$$

Figure 3.5 shows the energy transmission coefficient through a quarter-wavelength matching layer between quartz (typical transducer element) and water.

Of course, good matching is limited to the vicinity of the center frequency. The relative bandwidth (inverse quality factor) can be approximated as

$$\frac{1}{Q} = \frac{f_2 - f_1}{f_o} \approx \frac{4\sqrt{2r}}{\pi(r-1)} \approx \frac{1.8\sqrt{r}}{r-1}, \quad (3.27)$$

where  $f_1$  and  $f_2$  are the half-power (-6 dB) points. In the previously given example of quartz coupled to water, the relative bandwidth is reasonably wide at 69 %. In the case of larger impedance differences, the bandwidth where good transmission occurs is much lower. For example, Figure 3.6 shows the energy transmission coefficient through a quarter-wavelength matching layer between steel and water where the relative bandwidth is only 33 %.

It can be also seen from Equation 3.10 that whenever the layer thickness is equal to an integer multiple of the half-wavelength, i. e.,  $d = n\lambda/2$ , the input impedance is equal to the load impedance and the presence of the layer does not affect the transmission and reflection coefficients of the interface between the two surrounding media.

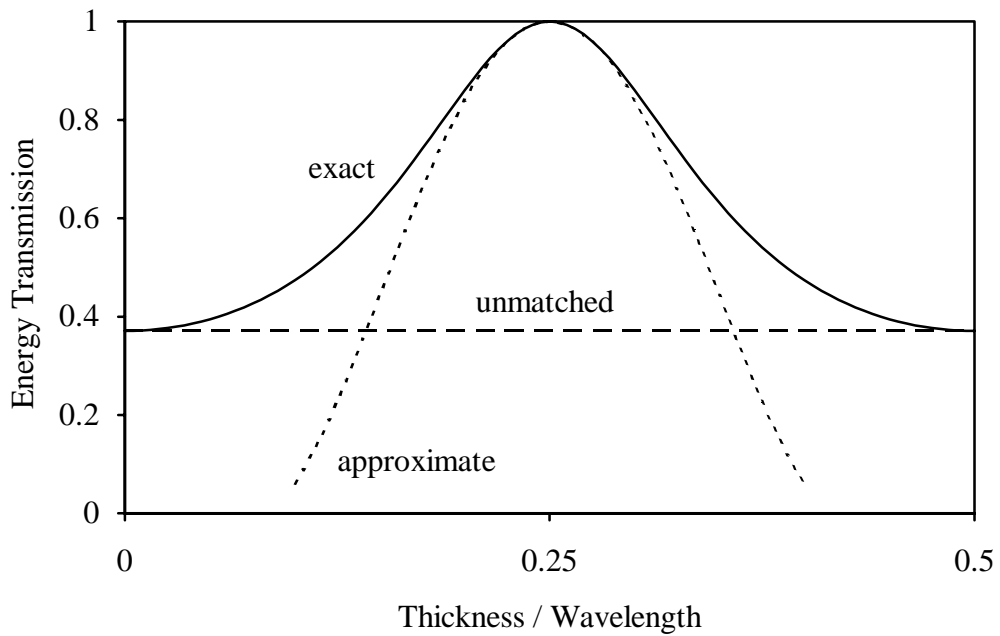


Figure 3.5 Energy transmission coefficient through a quarter-wavelength matching layer between quartz and water.

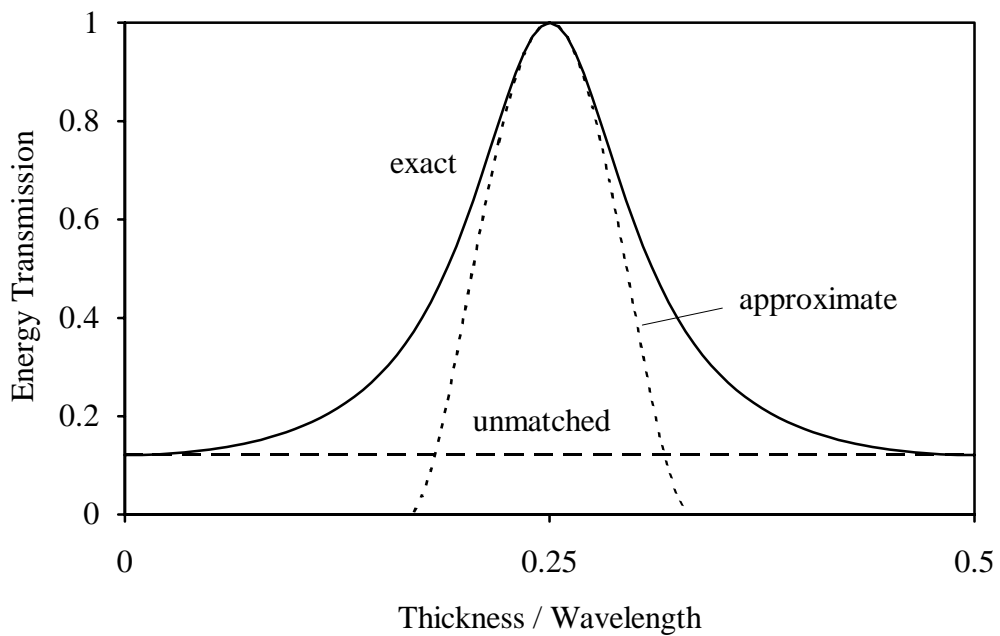


Figure 3.6 Energy transmission coefficient through a quarter-wavelength matching layer between steel and water.

### 3.2 Reflection/transmission - oblique incidence

A more general situation of reflection and transmission of waves at an interface occurs when the incident wave strikes at an oblique angle. A large number of possibilities exist, depending on the combinations of solid, fluid and vacuum of the two media and, if the incident media is a solid, whether the incident wave is pressure or shear wave. There are two somewhat opposite approaches to handle this complexity. One can start from the simplest case of longitudinal wave interaction with a fluid-fluid interface and build up build up the complexity step-by-step by introducing solid on one side then on the other. We shall follow another approach by giving formal solution for the most general solid-solid interface for an arbitrary incident wave then simplify the resulting formulas for the simpler cases. This approach was adapted from B. A. Auld *Acoustic Fields and Waves* (John Wiley & Sons, New York, 1973) Vol. II, pp. 21-38.

*General case:* In the most general case, either a longitudinal or a shear incident wave interacts with a solid-solid interface. This situation is shown in Figure 3.7.

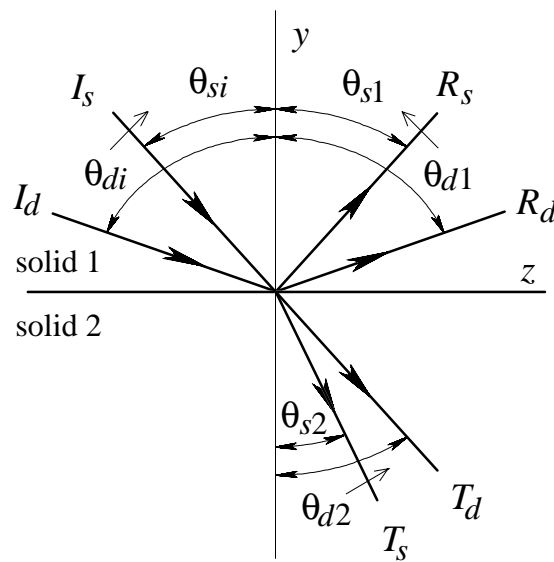


Figure 3.7 General acoustic wave interaction with a solid-solid interface.

From Snell's Law,

$$\frac{\sin \theta_{di}}{c_{d1}} = \frac{\sin \theta_{si}}{c_{s1}} = \frac{\sin \theta_{d1}}{c_{d1}} = \frac{\sin \theta_{s1}}{c_{s1}} = \frac{\sin \theta_{d2}}{c_{d2}} = \frac{\sin \theta_{s2}}{c_{s2}}. \quad (3.28)$$

The particle displacement amplitudes of the incident, reflected, and transmitted longitudinal waves are  $I_d$ ,  $R_d$ , and  $T_d$ , respectively. Similarly, the particle displacement amplitudes of the incident, reflected, and transmitted shear waves are  $I_s$ ,  $R_s$ , and  $T_s$ . Only two stress components are relevant to the boundary conditions:

$$\tau_{yy} = \lambda \frac{\partial u_z}{\partial z} + (\lambda + 2\mu) \frac{\partial u_y}{\partial y} \quad (3.29)$$

and

$$\tau_{zy} = \mu \left( \frac{\partial u_y}{\partial z} + \frac{\partial u_z}{\partial y} \right), \quad (3.30)$$

where  $\mu_1 = \rho_1 c_{s1}^2$ ,  $\lambda_1 + 2\mu_1 = \rho_1 c_{d1}^2$ ,  $\mu_2 = \rho_2 c_{s2}^2$ , and  $\lambda_2 + 2\mu_2 = \rho_2 c_{d2}^2$ .

The boundary conditions require that both normal and transverse velocity and stress components be continuous at the interface:

$$\begin{bmatrix} u_y^{(2)} - u_y^{(1)} \\ u_z^{(2)} - u_z^{(1)} \\ \tau_{yy}^{(2)} - \tau_{yy}^{(1)} \\ \tau_{zy}^{(2)} - \tau_{zy}^{(1)} \end{bmatrix} = \begin{bmatrix} 0 \\ 0 \\ 0 \\ 0 \end{bmatrix} \quad \text{or} \quad \begin{bmatrix} -u_y^{(d1)} + u_y^{(d2)} - u_y^{(s1)} + u_y^{(s2)} \\ -u_z^{(d1)} + u_z^{(d2)} - u_z^{(s1)} + u_z^{(s2)} \\ -\tau_{yy}^{(d1)} + \tau_{yy}^{(d2)} - \tau_{yy}^{(s1)} + \tau_{yy}^{(s2)} \\ -\tau_{zy}^{(d1)} + \tau_{zy}^{(d2)} - \tau_{zy}^{(s1)} + \tau_{zy}^{(s2)} \end{bmatrix} = \begin{bmatrix} u_y^{(i)} \\ u_z^{(i)} \\ \tau_{yy}^{(i)} \\ \tau_{zy}^{(i)} \end{bmatrix}, \quad (3.31)$$

where the incident wave can be either longitudinal ( $I_d = 1$ ,  $I_s = 0$ ) or shear ( $I_s = 1$ ,  $I_d = 0$ ).

Equation 3.31 can be written by using the displacement amplitudes as follows

$$\begin{bmatrix} a_{11} & a_{12} & a_{13} & a_{14} \\ a_{21} & a_{22} & a_{23} & a_{24} \\ a_{31} & a_{32} & a_{33} & a_{34} \\ a_{41} & a_{42} & a_{43} & a_{44} \end{bmatrix} \begin{bmatrix} R_d \\ T_d \\ R_s \\ T_s \end{bmatrix} = \begin{bmatrix} b_1 \\ b_2 \\ b_3 \\ b_4 \end{bmatrix} \quad \text{or} \quad \begin{bmatrix} c_1 \\ c_2 \\ c_3 \\ c_4 \end{bmatrix} \quad (3.32)$$

depending on whether longitudinal or shear wave incidence is considered. The matrix elements  $a_{ij}$ ,  $b_i$ , and  $c_i$  can be easily calculated from simple geometrical considerations:

$$\mathbf{a} = \begin{bmatrix} -\cos \theta_{d1} & -\cos \theta_{d2} & -\sin \theta_{s1} & \sin \theta_{s2} \\ -\sin \theta_{d1} & \sin \theta_{d2} & \cos \theta_{s1} & \cos \theta_{s2} \\ -Z_{d1} \cos 2\theta_{s1} & Z_{d2} \cos 2\theta_{s2} & -Z_{s1} \sin 2\theta_{s1} & -Z_{s2} \sin 2\theta_{s2} \\ -Z_{s1} \frac{c_{s1}}{c_{d1}} \sin 2\theta_{d1} & -Z_{s2} \frac{c_{s2}}{c_{d2}} \sin 2\theta_{d2} & Z_{s1} \cos 2\theta_{s1} & -Z_{s2} \cos 2\theta_{s2} \end{bmatrix} \quad (3.33)$$

For brevity, the common  $-i\omega$  factor was omitted in the last two rows. (The sign of all elements in the third column of matrix  $\mathbf{a}$  has been changed with respect to Auld's results to account for the opposite polarization of the reflected shear wave in his book.)

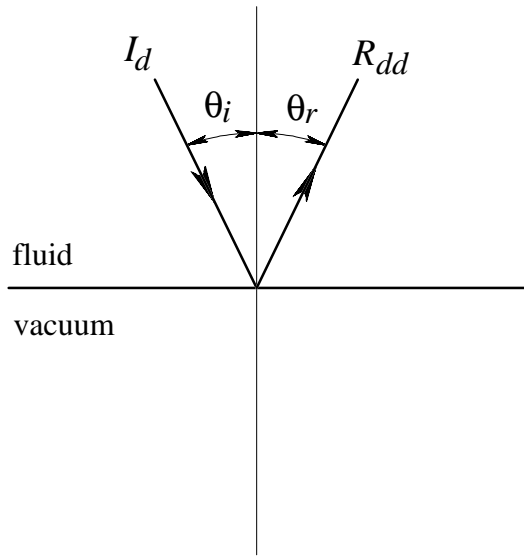
$$\mathbf{b} = \begin{bmatrix} -\cos \theta_{di} \\ \sin \theta_{di} \\ Z_{d1} \cos 2\theta_{si} \\ -Z_{s1} \frac{c_{s1}}{c_{d1}} \sin 2\theta_{di} \end{bmatrix} \quad \text{and} \quad \mathbf{c} = \begin{bmatrix} \sin \theta_{si} \\ \cos \theta_{si} \\ -Z_{s1} \sin 2\theta_{si} \\ -Z_{s1} \cos 2\theta_{si} \end{bmatrix} \quad (3.34)$$

The reflection and transmission coefficients can be determined by applying the well-known Cramer's rule.

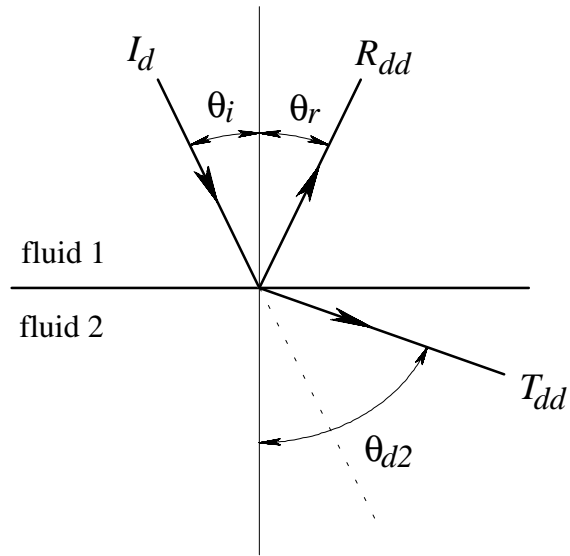
$$R_d = \frac{\det[\mathbf{a}^{(1)}]}{\det[\mathbf{a}]}, \quad T_d = \frac{\det[\mathbf{a}^{(2)}]}{\det[\mathbf{a}]}, \quad R_s = \frac{\det[\mathbf{a}^{(3)}]}{\det[\mathbf{a}]}, \quad T_s = \frac{\det[\mathbf{a}^{(4)}]}{\det[\mathbf{a}]}, \quad (3.35)$$

where  $\mathbf{a}^{(i)}$  is the matrix obtained by replacing the  $i$ th column of  $\mathbf{a}$  by either  $\mathbf{b}$  or  $\mathbf{c}$  vectors depending on whether longitudinal or shear incidence is used. It will be possible to give only a few specific results, with just the general behavior outlined for most cases. Figure 3.8a-d shows the schematic diagrams of reflection and transmission of waves for various combinations of materials. In these figures and in the following, the first index of the reflection and transmission coefficients indicate the type of the incident wave. For example,  $R_{sd}$  is the dilatational reflection coefficient for shear wave incidence and  $T_{dd}$  is the dilatational transmission coefficient for dilatational wave incidence.

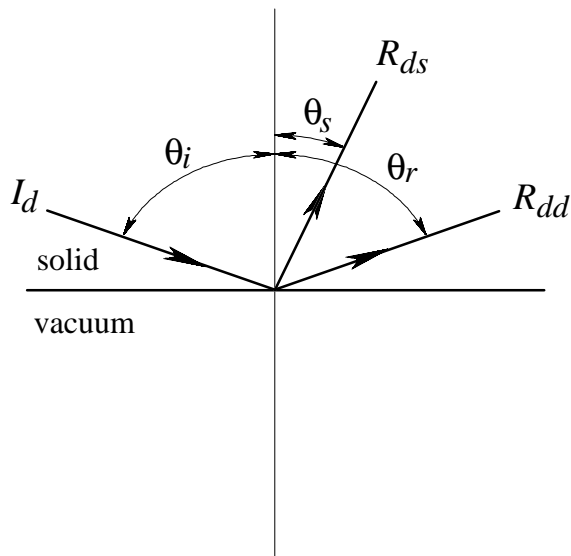
a) fluid-vacuum



b) fluid-fluid ( $c_{d2} > c_{d1}$ )



c) solid-vacuum  
(longitudinal incidence)



d) solid-vacuum  
(shear incidence)

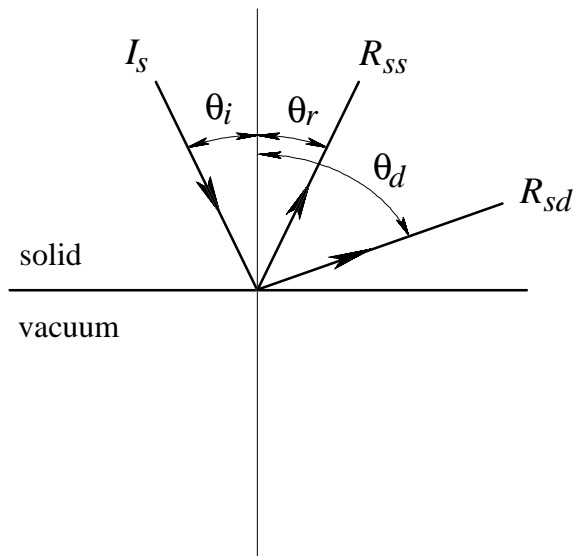
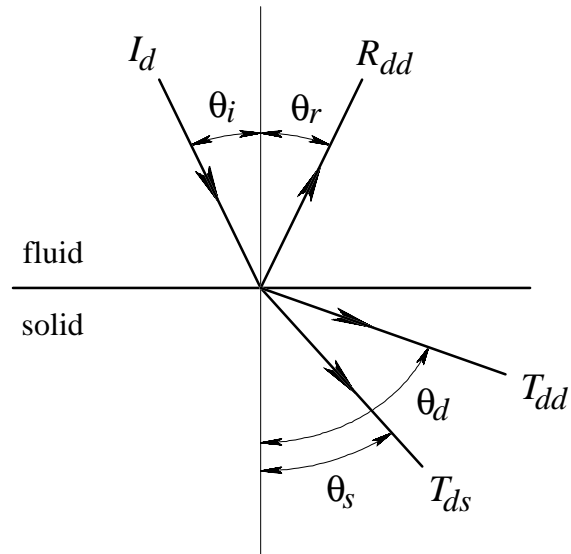


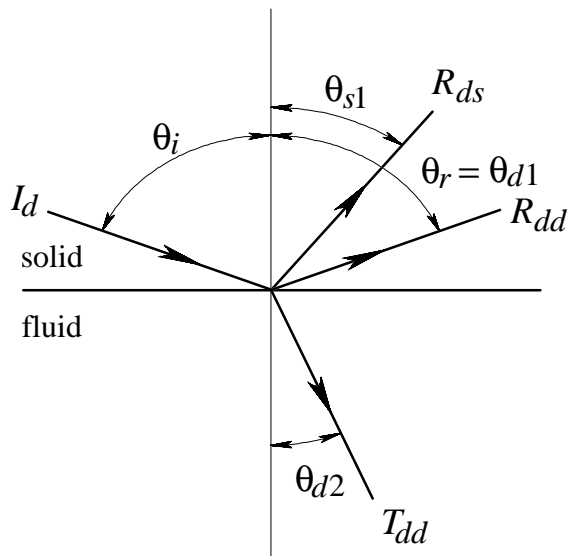
Figure 3.8a-d

Reflection and transmission of waves for various combinations of materials.

e) fluid-solid



f) solid-fluid  
(longitudinal incidence)



g) solid-fluid  
(shear incidence)

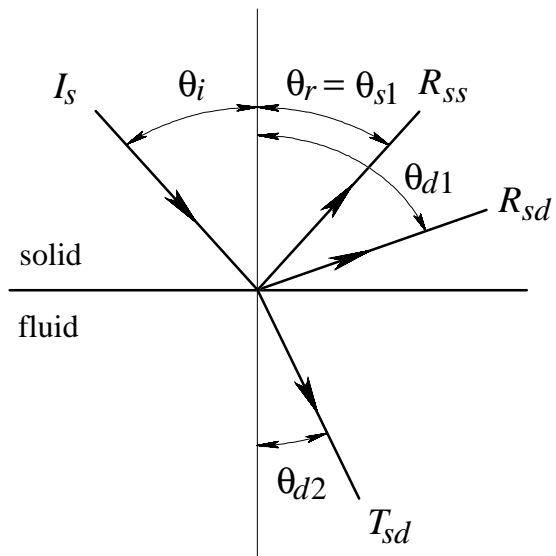
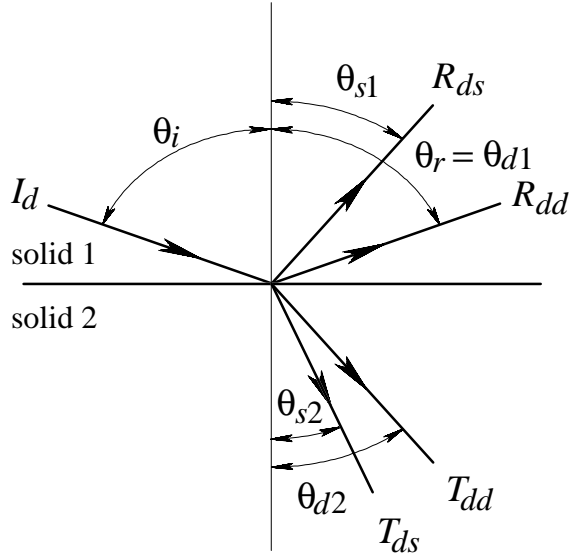


Figure 3.8e-g

Reflection and transmission of waves for various combinations of materials.



h) solid-solid  
(longitudinal incidence)



i) solid-solid  
(shear incidence)

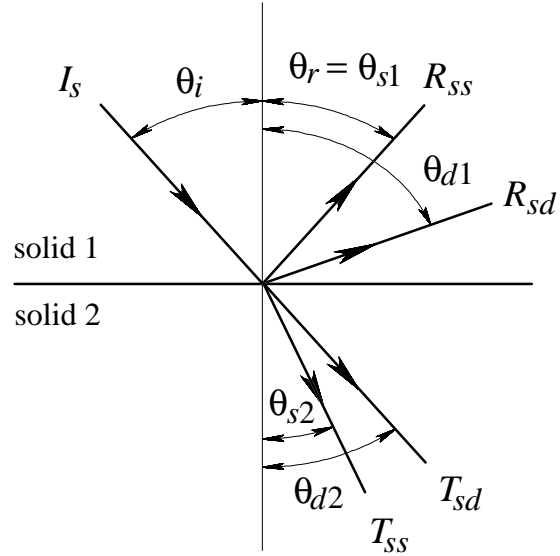


Figure 3.8h-i Reflection and transmission of waves for various combinations of materials.

The simplest situation of a fluid-vacuum boundary will be considered first.

*Fluid-vacuum:* The case of a pressure wave incident on a fluid-vacuum interface is shown in Fig. 3.8a. This is the simplest reflection case and results in

$$R_{dd} \equiv 1, \quad \theta_r = \theta_i. \quad (3.36)$$

*Fluid-fluid:* Two fluid media in contact result in a reflected and a transmitted (or refracted) wave. The relationships governing the angles are (Snell's law):

$$\theta_r = \theta_i, \quad \frac{\sin \theta_{d2}}{c_{d2}} = \frac{\sin \theta_i}{c_{d1}}. \quad (3.37)$$

From the second equation, we have

$$\sin \theta_{d2} = \frac{c_{d2}}{c_{d1}} \sin \theta_i . \quad (3.38)$$

This leads to the conclusion that if

$$c_{d2} < c_{d1} \quad \text{then} \quad \theta_{d2} < \theta_i \quad (3.39)$$

and if

$$c_{d2} > c_{d1} \quad \text{then} \quad \theta_{d2} > \theta_i . \quad (3.40)$$

In Figure 3.8b, the dashed line in media 2 is at the incidence angle. When medium 2 is "slower" than medium 1, the refracted wave is bent or steered toward the normal. When medium 2 is "faster" than medium 1 (which is the case illustrated), the wave is bent toward the surface.

It may be also seen from (3.31) that for a given ratio of  $c_{d2}/c_{d1}$ , there will exist an angle  $\theta_{ic}$  (critical angle) for which  $\sin \theta_{d2} \rightarrow 1$ ,  $\theta_{d2} \rightarrow 90^\circ$ . Thus, the refracted wave is parallel to the interface. For any angle beyond the critical angle, *total reflection* of the incident wave occurs.

*Solid-vacuum:* Since the incident wave is in a solid medium, it may be either pressure (Fig. 3.8c) or shear (Fig. 3.8d). The most remarkable feature of this and other cases involving solid media is the phenomenon of *mode conversion*. What occurs is that a P-wave generates both a P-wave and an S-wave upon reflection. Similar mode conversion can also occur in the case of an incident shear wave. The angular relations are as follows:

$$\text{P-wave incident:} \quad \theta_r (= \theta_d) = \theta_i, \quad \frac{\sin \theta_s}{c_s} = \frac{\sin \theta_i}{c_d} \quad (3.41)$$

$$\text{S-wave incident:} \quad \theta_r (= \theta_s) = \theta_i, \quad \frac{\sin \theta_d}{c_d} = \frac{\sin \theta_i}{c_s} . \quad (3.42)$$

For the case of an incident shear wave, it may be seen that there will again exist a critical value of the incidence angle for which  $\sin \theta_d \rightarrow 1$ , or  $\theta_d \rightarrow 90^\circ$ . This will inevitably occur since

$c_d > c_s$  always. For an incident angle beyond the critical angle, total reflection occurs for the shear wave and the reflected P-wave completely disappears.

We shall use this simple case as an example to demonstrate how to obtain the reflection and transmission coefficients from the previously given general formulas of Eqs. 3.31-3.35. In the case of a free solid surface, the boundary conditions require that both normal and transverse stress disappear at the surface but do not put any limitation of the particle displacement. At the same time, there are no transmitted shear or longitudinal waves to take into account at the boundary. Consequently, the first two rows and the second and fourth columns of the  $\mathbf{a}$  matrix given in Eq. 3.33 can be eliminated and we get a 2-by-2 matrix. For longitudinal incidence:

$$\begin{bmatrix} -Z_d \cos 2\theta_s & -Z_s \sin 2\theta_s \\ -Z_s \frac{c_s}{c_d} \sin 2\theta_d & Z_s \cos 2\theta_s \end{bmatrix} \begin{bmatrix} R_{dd} \\ R_{ds} \end{bmatrix} = \begin{bmatrix} Z_d \cos 2\theta_s \\ -Z_s \frac{c_s}{c_d} \sin 2\theta_d \end{bmatrix}. \quad (3.43)$$

By using Cramer's rule, the longitudinal-to-longitudinal reflection coefficient of the free solid surface can be obtained as

$$R_{dd} = -\frac{\cos^2 2\theta_s - \frac{c_s^2}{c_d^2} \sin 2\theta_s \sin 2\theta_d}{\cos^2 2\theta_s + \frac{c_s^2}{c_d^2} \sin 2\theta_s \sin 2\theta_d}, \quad (3.44)$$

which depends on the Poisson ratio of the solid only and  $R_{dd}(0^\circ) = R_{dd}(90^\circ) = -1$ . Naturally, the longitudinal-to-shear as well as the shear-to-longitudinal and the shear-to-shear wave reflection coefficients can be calculated in the same way.

Specific mathematical formulas have been obtained for the amplitudes of the reflected waves, with the results presented in a number of ways. Basically, the reflection behavior is dependent on incidence angle and material properties (specifically, Poisson's ratio). One illustration of this is given in Fig. 3.9 for the case of a solid-vacuum interface. In the case of shear wave incidence (Fig. 3.9b), the critical angle occurs where the  $R_{ss}$  becomes -1. Beyond the critical angle,  $R_{ss} \equiv -1$  and the reflected dilatational wave is evanescent. Another useful representation of this type of data is by a polar plot shown in Fig. 3.10 for  $\nu = 0.3$ .

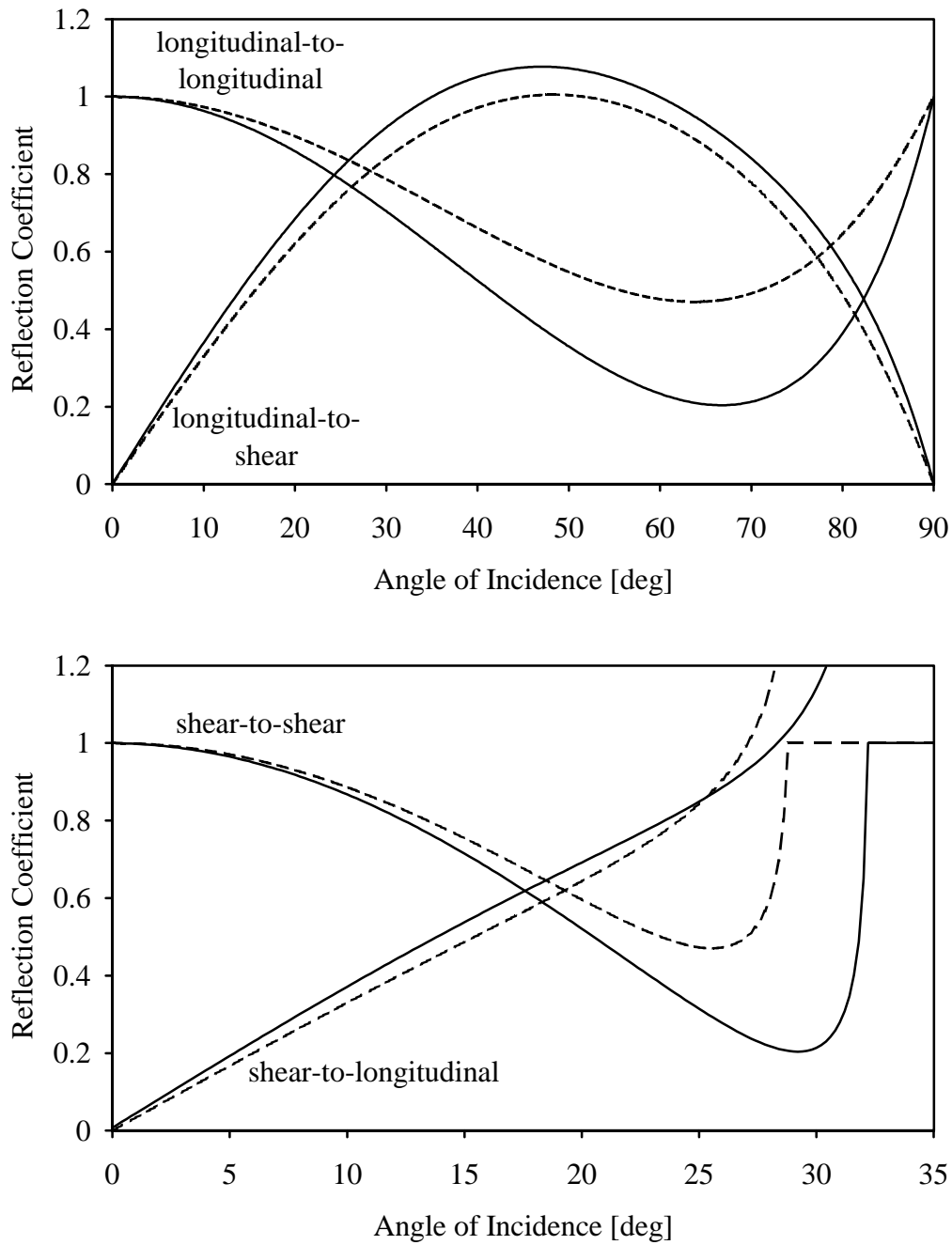


Figure 3.9 Absolute values of the longitudinal and shear wave reflection coefficients from a solid-vacuum interface as functions of the angle of incidence for two different Poisson's ratios (solid lines:  $\nu = 0.3$ , dashed lines:  $\nu = 0.35$ ).

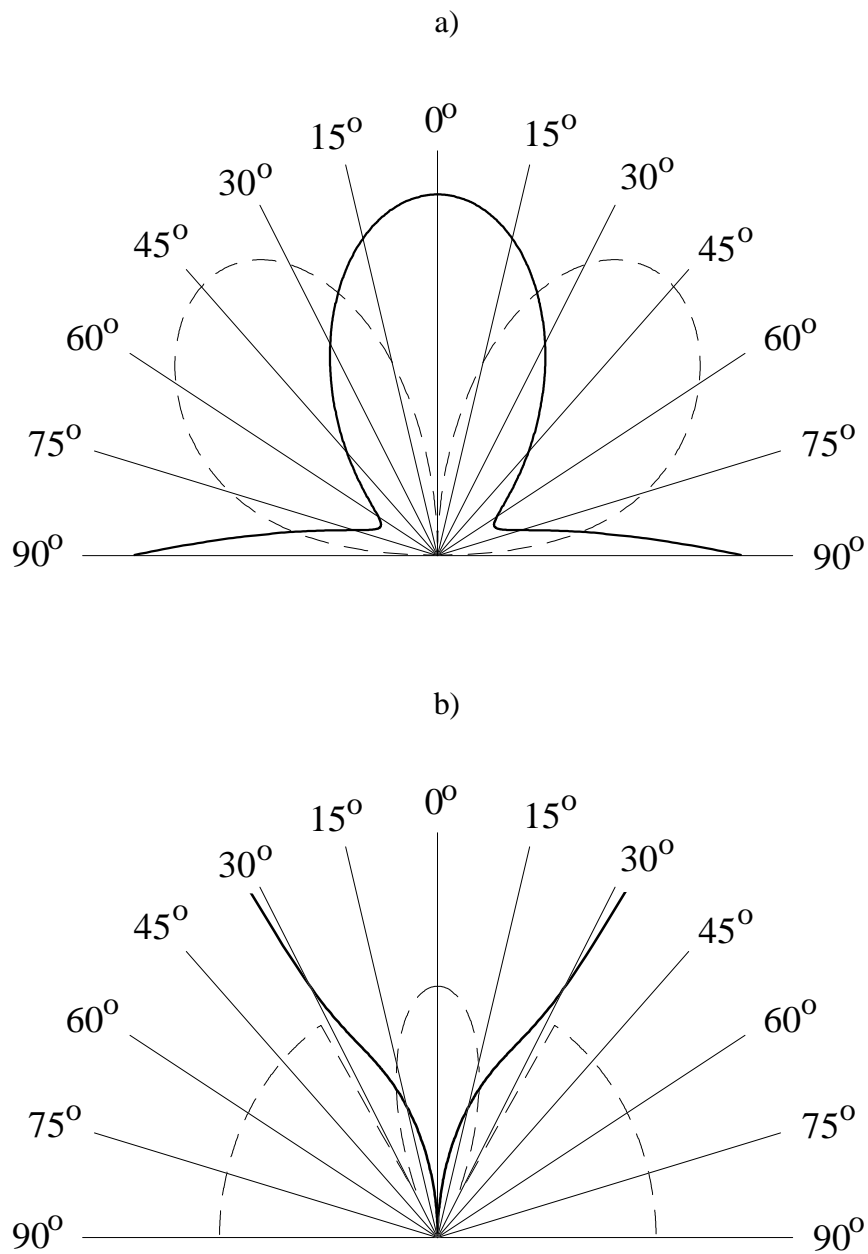


Figure 3.10 Polar diagram of the longitudinal (solid line) and shear (dashed line) wave reflection coefficients from a solid-vacuum interface in the case of (a) longitudinal and (b) shear incident waves ( $\nu = 0.3$ ).

### ***Displacement, stress, intensity, and power coefficients***

The reflection and transmission coefficients determined from Eq. (3.32) denote displacement ratios (without explicitly indicating it). In many cases, it is necessary to express the relative strength of the reflected and transmitted waves in terms of stress, intensity, or power. The stress coefficients can be obtained from the corresponding displacement coefficients by accounting for the impedance differences as follows:

$$\Gamma_{\alpha\beta}^{(stress)} = \Gamma_{\alpha\beta}^{(displacement)} \frac{Z_{\beta j}}{Z_{\alpha 1}} \quad \text{or simply,} \quad \Gamma_{\alpha\beta}^{(stress)} = \Gamma_{\alpha\beta} \frac{Z_{\beta j}}{Z_{\alpha 1}} \quad (3.45)$$

where  $\Gamma$  stands for either  $R$  ( $j = 1$ ) or  $T$  ( $j = 2$ ), and  $\alpha$  and  $\beta$  are either  $d$  or  $s$ . For propagating modes, the intensity coefficients then can be easily calculated as a product of the corresponding displacement and stress coefficients:

$$\Gamma_{\alpha\beta}^{(intensity)} = \Gamma_{\alpha\beta}^{(displacement)} \Gamma_{\alpha\beta}^{(stress)} = \Gamma_{\alpha\beta}^2 \frac{Z_{\beta j}}{Z_{\alpha 1}}, \quad (3.46)$$

Finally, for propagating modes the power coefficients can be obtained from the corresponding intensity coefficients by accounting for the different refraction angles as follows:

$$\Gamma_{\alpha\beta}^{(power)} = \Gamma_{\alpha\beta}^{(intensity)} \frac{\cos\theta_{\beta j}}{\cos\theta_{\alpha 1}} = \Gamma_{\alpha\beta}^2 \frac{Z_{\beta j}}{Z_{\alpha 1}} \frac{\cos\theta_{\beta j}}{\cos\theta_{\alpha 1}}. \quad (3.47)$$

It should be mentioned that the power coefficients are identically zero for evanescent waves, which do not carry energy away from the interface. The law of energy conservation can be written as follows:

$$R_{\alpha d}^{(power)} + R_{\alpha s}^{(power)} + T_{\alpha d}^{(power)} + T_{\alpha d}^{(power)} \equiv 1. \quad (3.48)$$

The law of reciprocity can be written as follows:

$$\Gamma_{\alpha\beta}^{(power)} \equiv \Gamma_{\beta\alpha}^{(power)}. \quad (3.49)$$

*Fluid-solid:* This case shown in Fig. 3.8d is of great interest when the fluid is liquid. Figure 3.11 shows the energy reflection and transmission coefficients for two cases of particular importance, i. e., for aluminum and steel immersed in water. Generally the transmission is much higher from water into aluminum than into steel, which is caused by the more than eight times higher density of the latter. Note that there is a wide range of incidence angle above the second (shear) critical angle for which the water wave is completely reflected. Of course there is no transmission into the shear component at normal incidence. The longitudinal transmission disappears above the first critical angle which is approximately  $13.5^\circ$  for aluminum. At this angle, the transmitted longitudinal wave propagates along the surface. At higher angles, the longitudinal transmitted wave is evanescent and does not carry energy away the interface.

*Solid-fluid:* Two cases may arise here, that of an incident P-wave, and an incident S-wave, as shown in Figs. 3.8f and g. Again, this is of great interest when the fluid is a liquid. The specific case of an aluminum/water interface is shown in Fig. 3.12. It is very important to realize that, according to the Reciprocity Theorem, the energy transmission coefficients are the same for the fluid-solid and the corresponding solid-fluid interfaces. For example, at  $18^\circ$  angle of incidence, the energy transmission coefficient from water into aluminum is 45.7 %, and the refraction angle of the shear wave is  $39.4^\circ$ . At the same  $39.4^\circ$  angle of incidence, the energy transmission coefficient of the aluminum-water interface for an incident shear wave is also 45.7 % and the compressional wave in the water is refracted at  $18^\circ$ .

*Solid-solid:* This situation is complicated by the fact that the two media may be solidly bonded together, or there may be a lubricated interface. The nature of distinction between the two situations is that for a bonded interface, both the normal and shear stresses must match at the interface. For a lubricated, or so-called slip, interface, it is only the normal stress and normal displacement that must match. It should be noted that the angles of reflection and transmission are not changed by the interface condition, only the various wave amplitudes are affected. The specific case of a Plexiglas/aluminum combination is shown in Fig. 3.12. The behavior in Fig. 3.12 is somewhat complicated because of the four possible secondary waves generated by mode conversion. The first critical angle,  $\theta_i = 25.6^\circ$ , is the angle at which the transmitted (or refracted) longitudinal wave disappears. The second critical angle,  $\theta_i = 62.4^\circ$ , corresponds to the angle of total reflection of the incident wave. Above this angle, all incident energy is reflected either as a longitudinal wave or as a mode-converted shear wave. Between  $25.6^\circ$  and  $62.4^\circ$ , one has a method of generating (just) shear waves in steel. This technique of assuring a single transmitted wave by working above the first critical angle is often used in everyday NDE.

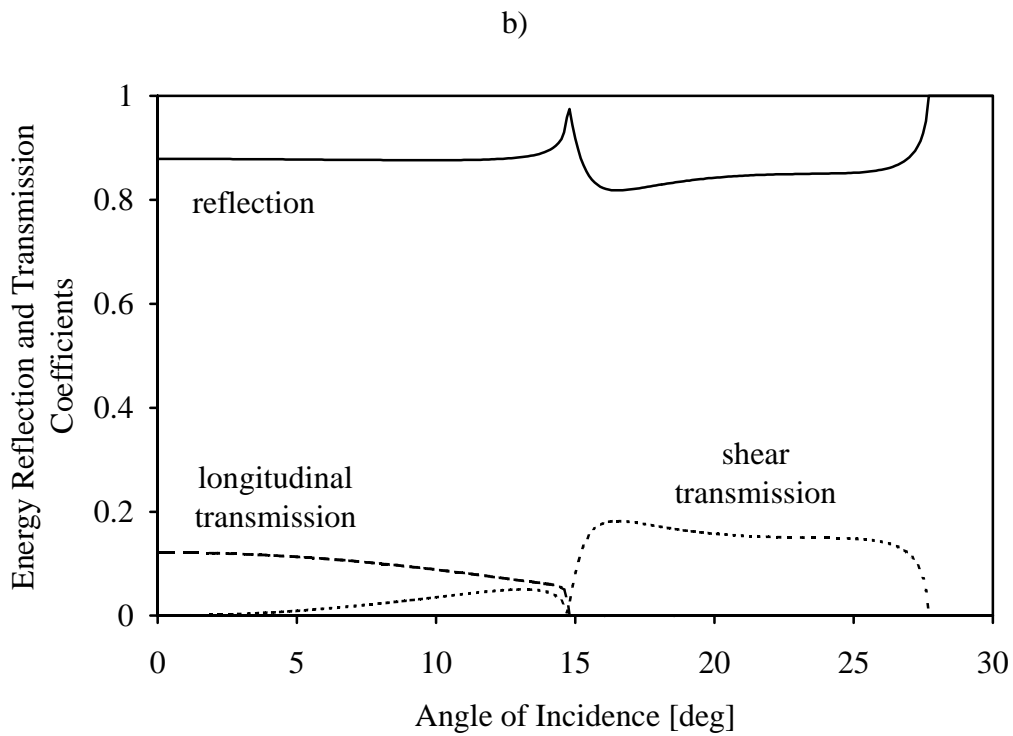
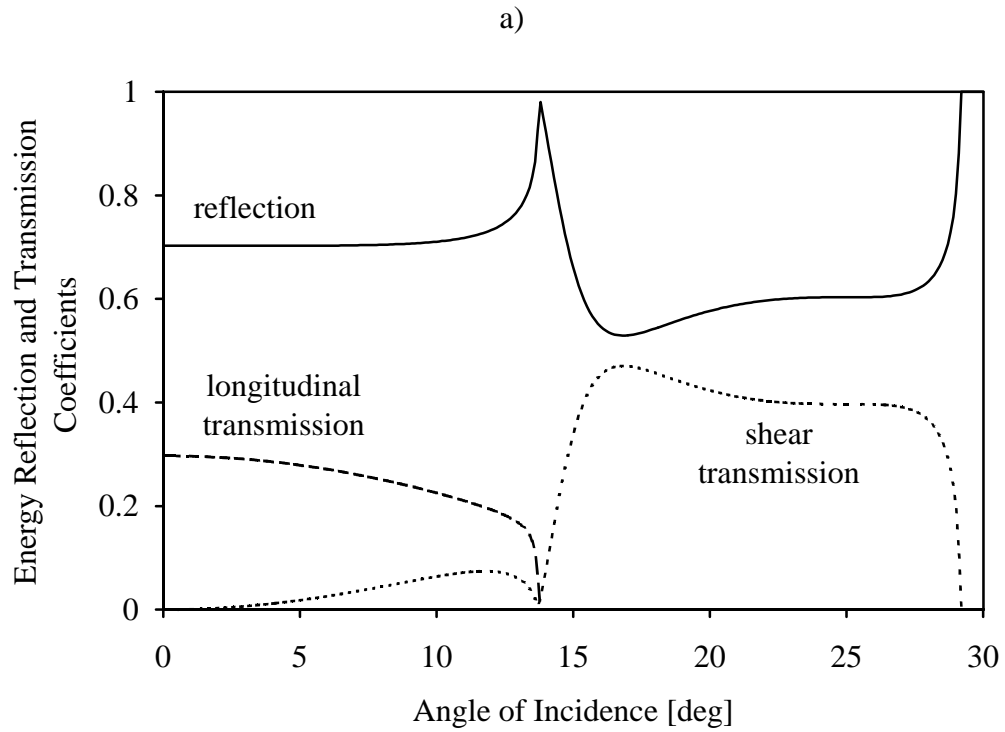


Figure 3.11 Energy reflection and transmission coefficients for (a) aluminum and (b) steel immersed in water.



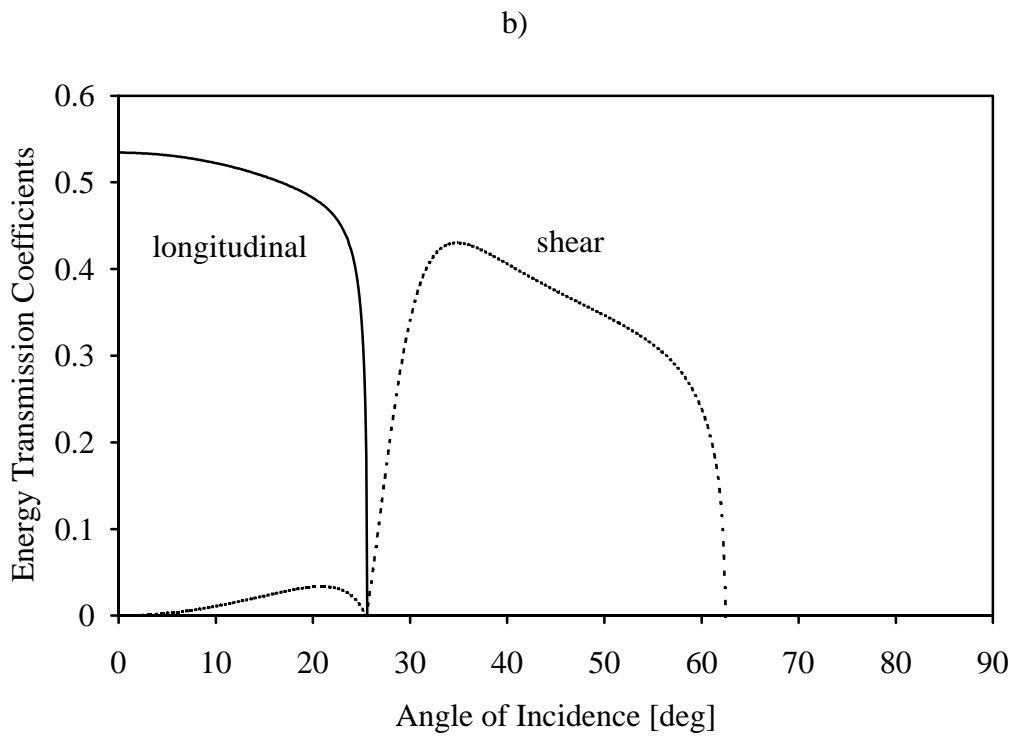
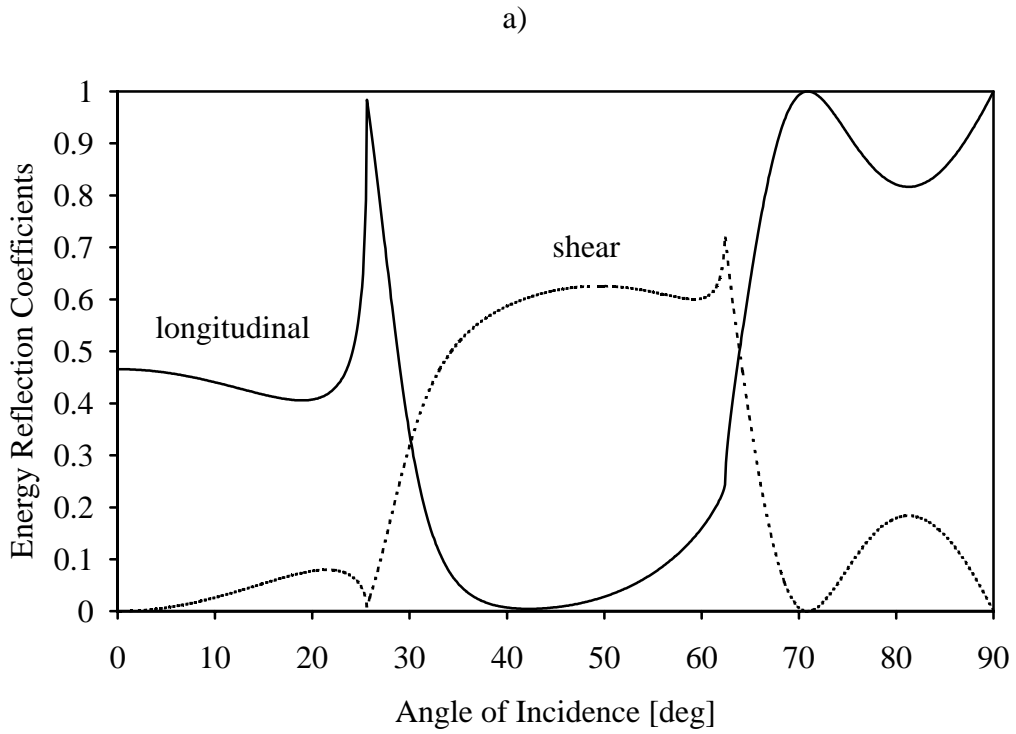


Figure 3.12 Energy (a) reflection and (b) transmission coefficients for a Plexiglas/aluminum interface in the case of longitudinal incidence.

### **Rayleigh wave**

Another interesting application of Eq. (3.43) is to derive the characteristic equation of the free vibration (as opposed to forced vibrations) of a solid-vacuum interface (free surface). The free vibration has to satisfy the homogeneous equation of

$$\begin{bmatrix} -Z_d \cos 2\theta_s & -Z_s \sin 2\theta_s \\ -Z_s \frac{c_s}{c_d} \sin 2\theta_d & Z_s \cos 2\theta_s \end{bmatrix} \begin{bmatrix} R_d \\ R_s \end{bmatrix} = \begin{bmatrix} 0 \\ 0 \end{bmatrix} \quad (3.50)$$

The mathematical condition on the existence of a nontrivial solution (the trivial solution is  $R_d = R_s = 0$ ) is that the determinant, i. e., the denominator of Eq. (3.50) be zero:

$$\cos^2 2\theta_s + \frac{c_s^2}{c_d^2} \sin 2\theta_s \sin 2\theta_d = 0. \quad (3.51)$$

Later we shall show that this is the characteristic equation of the well-known Rayleigh wave with sound velocity  $c_R$  lower than both shear and longitudinal wave velocities in the unbounded solid:

$$\frac{\sin \theta_s}{c_s} = \frac{\sin \theta_d}{c_d} = \frac{1}{c_R}. \quad (3.52)$$

Relative velocities:

$$\xi = \frac{c_s}{c_d} \quad \left( = \sqrt{\frac{1-2\nu}{2(1-\nu)}} \right) \quad (3.53)$$

$$\eta = \frac{c_R}{c_s} \quad (3.54)$$

Exact Rayleigh equation:

$$\eta^6 - 8\eta^4 + 8(3-2\xi^2)\eta^2 - 16(1-\xi^2) = 0 \quad (3.55)$$

Approximate expression

$$\eta \approx \frac{0.87+1.12\nu}{1+\nu} \quad (3.56)$$

*Longitudinal incident wave:* Suppose the P-wave is incident at  $50^\circ$  ( $\theta_d = \theta_i = 50^\circ$ ). Then the reflected P-wave has an amplitude of 0.35% and negative phase ( $\nu = 0.3$ ).  $\theta_s$  can be readily calculated from

$$\sin \theta_s = \frac{c_s}{c_d} \sin \theta_i = 0.55 \sin 50^\circ = 0.41 \text{ which yields } \theta_s = 24.2^\circ$$

and the shear wave reflection coefficient is -1.08 (since the shear wave impedance is much lower than the longitudinal one, the displacement amplitude of the reflected shear wave can be higher than the amplitude of the incident longitudinal wave) It is worthwhile to mention, that the phase of the reflected shear wave includes an arbitrary  $180^\circ$  component depending on the choice of the coordinate system.

*S wave incident.* Suppose  $\theta_s = \theta_i = 20^\circ$  again. Then the shear-to-shear reflection coefficient is  $R_s \approx 0.69$  and  $\theta_d$  can be determined from

$$\sin \theta_d = \frac{c_d}{c_s} \sin \theta_s \rightarrow \theta_d = 38.5^\circ.$$

The shear-to-longitudinal reflection coefficient is  $R_d \approx -0.53$ . Note that the critical angle of incidence of the shear wave is  $32.3^\circ$  and beyond that angle, there is no reflected pressure wave.